PHYSICAL REVIEW C VOLUME 40, NUMBER 1 JULY 1989

Reaction mechanisms in $^{28}Si+^{24}Mg \rightarrow \alpha+^{24}Mg+^{24}Mg$ and $\alpha+^{20}Ne+^{28}Si$

A. H. Wuosmaa, S. F. Pate,* and R. W. Zurmühle
Physics Department, University of Pennsylvania, Philadelphia, Pennsylvania 19104
(Received 9 March 1989)

We have studied the $^{28}Si+^{24}Mg$ system leading to the three-body final states $\alpha+^{24}Mg+^{24}Mg$ and $\alpha+^{20}Ne+^{28}Si$. Full momentum reconstruction on an event by event basis allows us to obtain all kinematic quantities, and perform a comparison of competing reaction mechanisms. A search reveals very little evidence for the population of high-spin states in ^{48}Cr corresponding to resonances observed in the $^{24}Mg+^{24}Mg$ system, via the $^{24}Mg(^{28}Si,\alpha)^{48}Cr^*(^{24}Mg)$ and $^{24}Mg(^{28}Si,\alpha)^{48}Cr^*(^{20}Ne)$ reactions. Instead, we find that the dominant processes that occur involve inelastic heavy-ion scattering to α-particle unbound states in ^{28}Si and ^{24}Mg.

Since the discovery of resonance behavior in systems with composite mass in the region $A\sim50$, much effort has gone into elucidating the systematics of these states. Strongly correlated peaks in the excitation functions for elastic and inelastic scattering of three sets of α-particle nuclei have now been observed, in the $^{24}Mg+^{24}Mg$, $^{28}Si+^{28}Si$, and $^{24}Mg+^{28}Si$ systems.[1–4] These resonances correspond to long-lived ($\Gamma_{c.m.}\sim150$ keV), high-spin levels in the composite systems ^{48}Cr, ^{56}Ni, and ^{52}Fe. For the inelastic scattering of $^{24}Mg+^{24}Mg$, particle-γ angular-correlation measurements have yielded a spin assignment of $J^{\pi}=36^{+}$ for a resonance observed at $E_{c.m.}=45.70$ MeV.[5] The resonances in this system were also observed to have weak decay branches to the $^{20}Ne+^{28}Si$ final state.[6]

Attempts to extend such measurements to heavier α-particle systems have met with limited success. Studies of the elastic and inelastic scattering of $^{32}S+^{32}S$ and $^{40}Ca+^{40}Ca$ (Refs. 7 and 8) show no such resonance behavior. One problem encountered in the search for resonances involving heavier nuclei is that as the Coulomb barrier increases, the strong potential scattering background tends to obscure the presence of narrow states. Furthermore, it appears that the deformation of the nuclei in the entrance channel may play a role in the enhancement of those narrow structures above the background of direct inelastic scattering and compound-nuclear fluctuations. It is therefore difficult to discern whether properties of the composite system such as shell structure or deformation are also important ingredients for the existence of strong narrow resonances.

An answer to this question could possibly be provided if these states were observed as final states in a transfer reaction, rather than as resonances. Observation of fissioning high-spin states in such a transfer reaction would also present a new experimental vista for the study of similar states in heavier systems inaccessible via elastic and inelastic scattering.

We wished to apply these ideas to a system in which resonance behavior was well established. We chose to study the nucleus ^{48}Cr. In this nucleus, previous studies[1,2] have shown that there exist several prominent resonances in $^{24}Mg+^{24}Mg$ elastic scattering corresponding to states in ^{48}Cr between $E_x=60$ and 68 MeV. We chose to study the population of such high-spin levels in ^{48}Cr through the $^{24}Mg(^{28}Si,\alpha)^{48}Cr^*$ reaction. In order to isolate final states that might correspond to a fissioning high-spin ^{48}Cr nucleus, we required that the α particle be in coincidence with two heavy-ion fragments. In our experiment we used a three-detector coincidence setup to measure the energies of each particle in the final state, as well as the direction of the α particle. This measurement allows us to determine a complete set of three-body kinematic variables. We can then use the different kinematic signatures to distinguish between different competing reaction mechanisms. For instance, in the $^{24}Mg(^{28}Si,\alpha)^{48}Cr^*$ reaction, the α particle obeys two-body kinematics, while for an inelastic scattering process such as $^{24}Mg(^{28}Si,^{28}Si)^{24}Mg^*(\alpha)$, two-body kinematics are followed by the ^{28}Si nucleus.

Similar experiments have been performed in the past in attempts to study states in ^{24}Mg corresponding to resonances observed in elastic and inelastic $^{12}C+^{12}C$ scattering. Nagatani *et al.* reported evidence for the population of high-spin states in ^{24}Mg corresponding to these resonances via the $^{12}C(^{16}O,\alpha)^{2}Mg^*$ reaction.[9] Lazzarini *et al.* also studied this reaction, examining the $\alpha+^{12}C+^{12}C$ and $\alpha+^{8}Be+^{16}O$ final states,[10] and concluded that structure in the α-particle energy spectra could be associated with resonances observed in scattering of $^{12}C+^{12}C$.

Rather different pictures of these three-body reactions were offered by Rae, *et al.*,[11] and Wieland *et al.*[12] Rae *et al.*, also examined the $^{12}C(^{16}O,\alpha)^{24}Mg^*(^{12}C)$ and $^{13}C(^{16}O,\alpha)^{25}Mg^*(^{12}C)$ reactions, only to show that the dominant reaction mechanism was inelastic scattering to discrete, particle-unbound states in ^{16}O, followed by decay via α-particle emission. Little or no evidence was found for the population of fissioning, high-spin states in the composite nuclei ^{24}Mg and ^{25}Mg. A similar conclusion was reached by Wieland *et al.*, who noted a strong $\alpha+^{12}C$ final-state interaction in the $^{16}O+^{12}C\rightarrow\alpha+^{12}C+^{12}C$ reaction. In view of these somewhat contradictory results, we sought to determine which reaction mechanisms were at work in the $^{28}Si+^{24}Mg\rightarrow\alpha+^{24}Mg+^{24}Mg$ and $^{28}Si+^{24}Mg\rightarrow\alpha+^{20}Ne+^{28}Si$ systems. The experiment which we performed was sensitive to both types of final-state interactions.

We performed our experiment using 140 and 150 MeV

^{28}Si beams from the Brookhaven National Laboratory (BNL) Tandem Van de Graaff accelerator. We detected α particles in the range of $9° \leq \theta_{lab} \leq 26°$ using a position-sensitive telescope.[13] This device had a gas ionization chamber as a ΔE detector, and a position-sensitive solid state counter as an E detector. A thick (~ 15 μm) Ta foil was placed in front of the telescope entrance window to stop forward scattered heavy ions. We used α particles from the ^{12}C(^{12}C,α)^{24}Mg reaction to provide an energy calibration for this device. From our calibration data, we determined the energy resolution of this device to be between 250 and 300 keV. The dominant contribution to this resolution is straggling of α particles as they penetrate the Ta foil.

In coincidence with the α particles, we detected heavy-ion (HI) fragments with a setup analogous to a recoil coincidence arrangement using two large-area, high-resolution surface barrier detectors. One HI detector spanned 12.0° in the lab, and was centered at $\theta_{lab}=42°$ on the same side of the beam as the α-particle telescope. The HI detector on the opposite side of the beam was centered at 40° and spanned 26°. We used a small solid angle silicon detector centered at 10° to measure forward angle elastic scattering and monitor the condition of the target throughout the experiment. A schematic diagram of the particle detector setup appears in Fig. 1. Compact time-pickoff units affixed to each detector provided us with timing resolution sufficient to determine the time-of-flight difference (ΔTOF) between the HI reaction fragments ($\sim$250 ps). This measurement allowed us to obtain HI particle identification information.[4] The two HI energy signals, the α-particle position, energy and ΔE signals, and the two signals from the two time-to-amplitude converters (TAC's) were recorded event by event onto magnetic tape.

Figure 2 shows a two-dimensional HI particle identification spectrum for an energy of $E_{lab}=150$ MeV, where the heavy ions are in coincidence with an α particle. This spectrum is gated on a total reaction Q value of $Q_3=-10.0$ MeV. Several different heavy-ion groups are visible and clearly resolved. In particular, the central group corresponds to the $\alpha+{}^{24}$Mg$+{}^{24}$Mg exit channel. On either side lie events corresponding to the $\alpha+{}^{20}$Ne$+{}^{28}$Si exit channel. The weak groups at the edges of the display correspond to the $\alpha+{}^{16}$O$+{}^{32}$S final state. The timing resolution seen in this spectrum is approximately 250 ps full-width-half-maximum (FWHM). The bar in Fig. 2 corresponds to a ΔTOF of 1 ns.

Once the reaction fragments have been identified, the measurement of the α-particle energy and angle, and the energies of the two heavy ions allows us to reconstruct all of the kinematic quantities in the reaction. Of particular interest are the laboratory scattering angles of the HI fragments. From the angle dependence of the HI energies, we can distinguish inelastic scattering from direct population of states in ^{48}Cr. The possible reaction mechanisms which we will consider are as follows:

$$^{28}\mathrm{Si}+{}^{24}\mathrm{Mg}\rightarrow{}^{48}\mathrm{Cr}^*({}^{24}\mathrm{Mg}+{}^{24}\mathrm{Mg})+\alpha \quad (1)$$

or

$$^{28}\mathrm{Si}+{}^{24}\mathrm{Mg}\rightarrow{}^{48}\mathrm{Cr}^*({}^{20}\mathrm{Ne}+{}^{28}\mathrm{Si})+\alpha\ ,$$

$$^{28}\mathrm{Si}+{}^{24}\mathrm{Mg}\rightarrow{}^{28}\mathrm{Si}^*({}^{24}\mathrm{Mg}+\alpha)+{}^{24}\mathrm{Mg}\ , \quad (2)$$

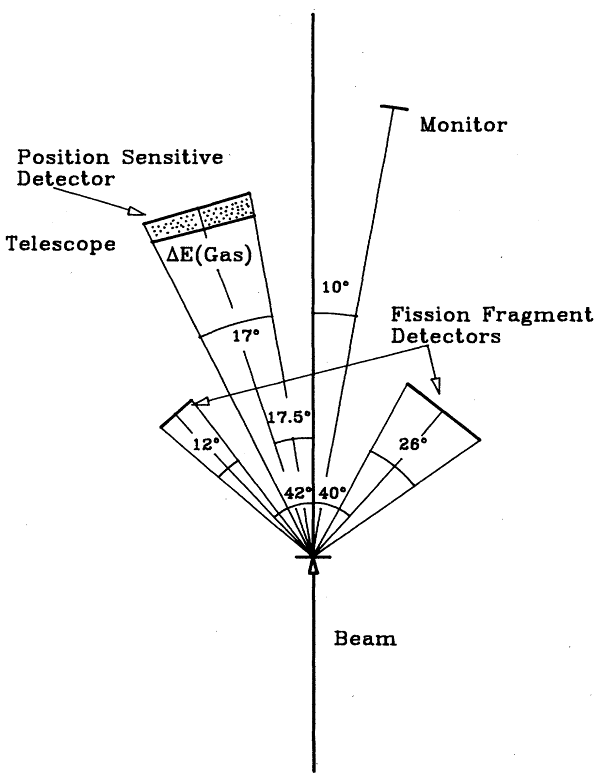

FIG. 1. Schematic diagram of the particle detector setup.

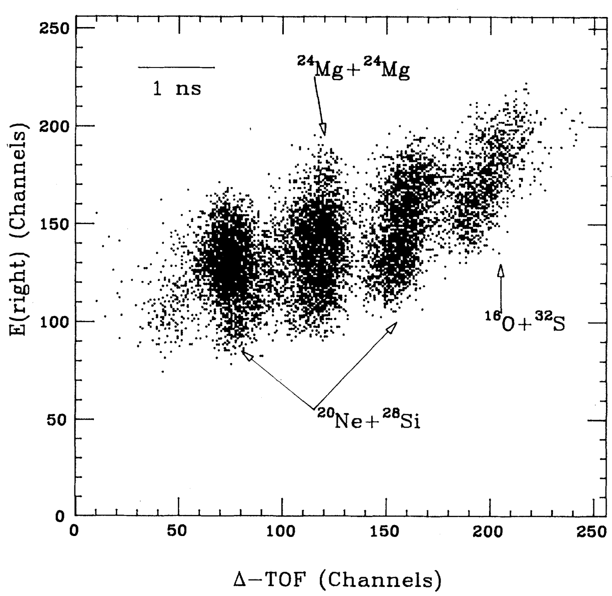

FIG. 2. Heavy-ion particle identification spectrum, for heavy ions in coincidence with an α particle. The central group corresponds to the $\alpha+{}^{24}$Mg$+{}^{24}$Mg channel. Adjacent and on either side are groups corresponding to $\alpha+{}^{20}$Ne$+{}^{28}$Si. The bar represents a ΔTOF of 1 ns.

and

$$^{28}\text{Si}+^{24}\text{Mg}\rightarrow^{24}\text{Mg}^*(^{20}\text{Ne}+\alpha)+^{28}\text{Si} \ . \quad (3)$$

In case (1), the excitation energy of the ^{48}Cr is determined from a simple function of the α-particle energy and angle $f(E_\alpha,\theta_\alpha)$. In cases (2) and (3), the excitation energy of the α-decaying heavy ion is determined from two-body kinematics using the energy and angle of the other heavy ion, i.e., $f(E_{^{24}\text{Mg}}\theta_{^{24}\text{Mg}})$ and $f(E_{^{28}\text{Si}},\theta_{^{28}\text{Si}})$ for cases (2) and (3), respectively. This method is similar to that of Dalitz,[14] and also similar to the analysis performed by Lazzarini *et al.*[10]

Figure 3 contains three-body Q-value spectra obtained at $E_{\text{lab}}=150$ MeV for the $\alpha+^{20}$Ne+^{28}Si and $\alpha+^{24}$Mg+^{24}Mg final states, obtained simply from summing the energies of the three detected particles. The ground-state Q values Q_{ggg} for these two reactions are -9.3135 MeV and -9.9815 MeV, respectively. Our analysis and particle identification technique is based upon the assumption of a three-body final state. Much of the cross section at large negative Q values corresponds to $N>3$- body final states. The highest Q value at which $N>3$-body final states can appear is $Q_3=-15.04$ MeV, which corresponds to the α-particle decay threshold for ^{20}Ne. Therefore, our particle identification is valid only for total reaction Q values of $Q_3>-15.04$ MeV.

In order to examine the different possible reaction mechanisms, we apply narrow gates on the total reaction Q value Q_3 to our data, to ensure that the heavy-ion fragments are only in either their ground or first-excited states (see Fig. 3). For case (1), this restriction is used, as the resonances seen in ^{24}Mg+^{24}Mg scattering have their largest decay branches to exit channels of low excitation energy in the ^{24}Mg+^{24}Mg system. For cases (2) and (3), restricting the excitation energy of the heavy ions in the

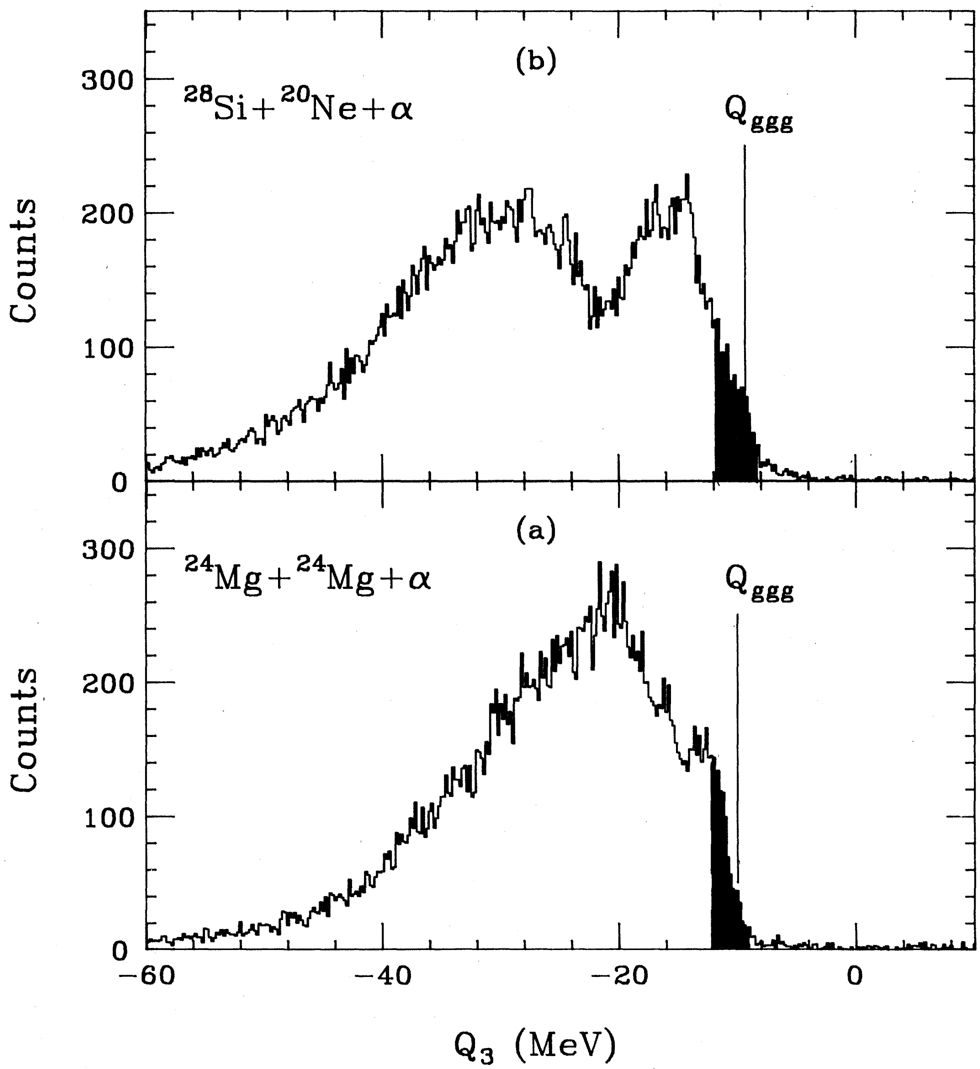

FIG. 3. Total reaction Q value Q_3 for (a) $\alpha+^{24}$Mg+^{24}Mg and (b) $\alpha+^{20}$Ne+^{28}Si final states. The lines indicate the ground state Q values Q_{ggg}=(a) -9.314 MeV and (b) -9.982 MeV. The darkened regions denote the range of the Q_3 gate used in the subsequent analysis.

final state limits the ambiguities inherent in determining the excitation energy of the α-decaying heavy ion.[15] For example, if we analyze our data in terms of an inelastic scattering mechanism, the two-body reaction Q value is given by

$$Q_2 = \frac{M_1+M_2}{M_2}E_1 - \frac{M_2-M_B}{M_2}E_B - \frac{2(M_B M_1 E_B E_1)^{1/2}}{M_2}\cos(\theta_1) ,$$

where B refers to the beam, and 1 and 2 refer to the detected and α-decaying heavy ions, respectively. For inelastic scattering, $Q_2 = -(E_{x1}+E_{x2})$. In order to unambiguously determine E_{x2} from (E_1,θ_1), we must ensure that particle 1, the detected heavy ion, is in its ground state. The resolution seen in the Q_3 spectra was not, however, sufficient to resolve closely spaced low-lying excitations. Also, as seen in Fig. 3, the statistics for these events are quite poor. As a compromise between excitation-energy ambiguity and statistics, for the inelastic scattering analysis we imposed the same Q_3 gate used in the $E_x(^{48}Cr)$ analysis.

Figure 4 shows spectra of excitation energy in ^{48}Cr coincident with the detection of two ^{24}Mg nuclei, at beam energies of 140 and 150 MeV. The inserts in Fig. 4 indicate the region of total reaction Q value Q_3 upon which the $E_x(^{48}Cr)$ spectra are gated. This range of Q_3, from $Q_3 = -8.8$ to -12.3 MeV, includes the 0^+-0^+, 0^+-2^+, and 2^+-2^+ excitations in $^{24}Mg+^{24}Mg$. It is in these low-lying excitations that the strongest resonance behavior is observed in $^{24}Mg+^{24}Mg$ scattering.[1,2] As already de-

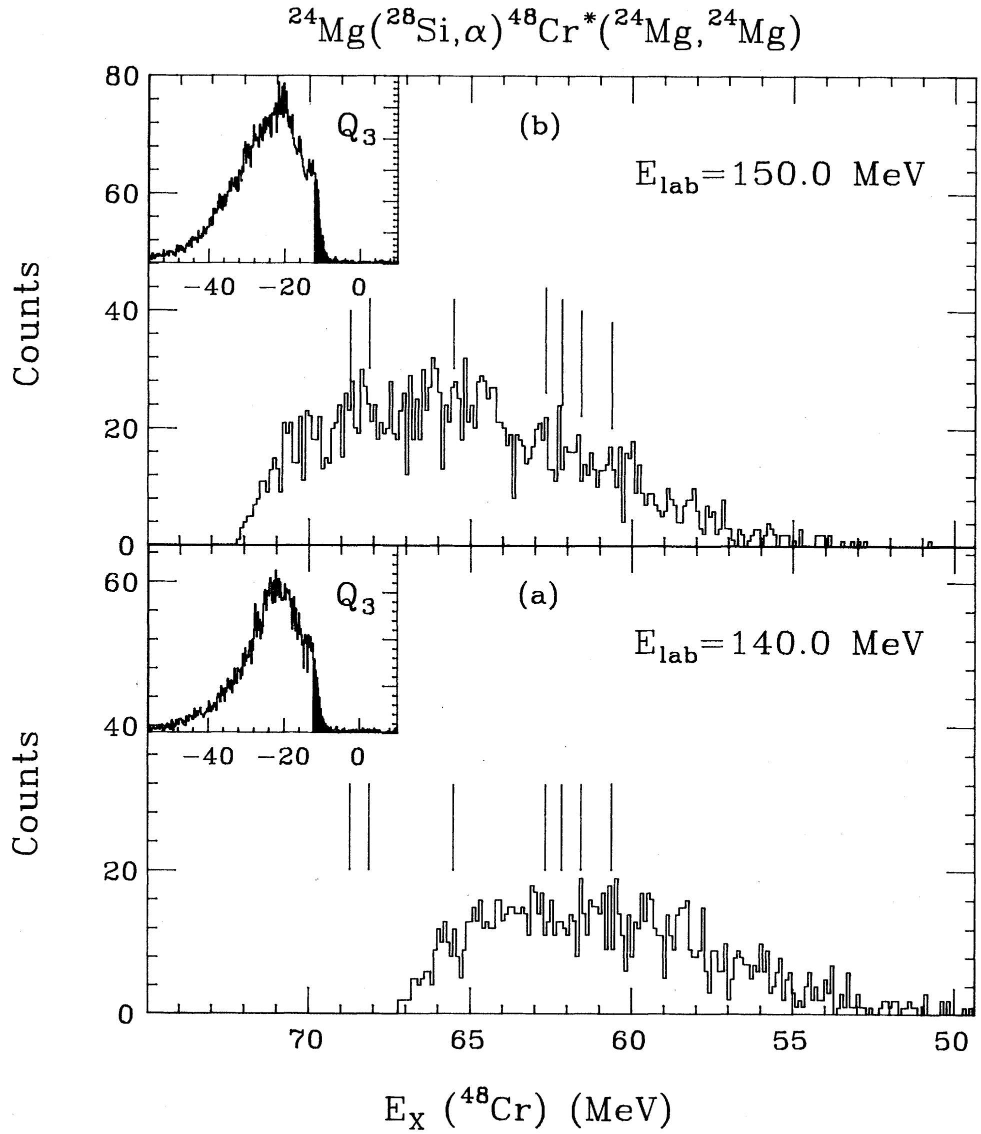

FIG. 4. Spectra of $E_x(^{48}Cr)$ derived from the energy and angle of α particles in coincidence with two ^{24}Mg nuclei. (a) $E_{lab}=140$ MeV. (b) $E_{lab}=150$ MeV. The inserts are the corresponding three-body Q-value spectra for the $\alpha+^{24}Mg+^{24}Mg$ reaction. The vertical lines in (b) at $E_x = 60.65$, 61.60, 62.20, 62.70, 65.55, 68.15, and 68.75 MeV indicate the excitation energies of resonances observed in $^{24}Mg+^{24}Mg$ elastic and inelastic scattering.

scribed, $E_x(^{48}\mathrm{Cr})$ is determined from (E_α,θ_α). The cutoffs at high excitation energy correspond to the lowest energy α particles that could penetrate the foil on the front of the α-particle telescope. The lines in Fig. 4(a) indicate the excitation energies for the resonances observed in $^{24}\mathrm{Mg}+^{24}\mathrm{Mg}$ elastic and inelastic scattering.

There is little evidence in these spectra for the population of fissioning, high-spin states in ^{48}Cr through the $^{24}\mathrm{Mg}(^{28}\mathrm{Si},\alpha)^{48}\mathrm{Cr}^*$ reaction. We see no strong enhancement of the cross section for regions of excitation energy corresponding to the energies of resonances observed in $^{24}\mathrm{Mg}+^{24}\mathrm{Mg}$ scattering. In particular, at $E_x(^{48}\mathrm{Cr}) = 65.55$ MeV, the excitation energy corresponding to a very strong, $\Gamma\sim400$ keV wide, resonance in $^{24}\mathrm{Mg}+^{24}\mathrm{Mg}$ scattering, we find no notable structure in the α-particle energy spectrum. We conclude that the cross section for the formation of such high-spin states in ^{48}Cr is quite small, below the level of sensitivity in our experiment. Figure 5 contains corresponding $E_x(^{48}\mathrm{Cr})$ spectra, where the α particle is now in coincidence with $^{20}\mathrm{Ne}+^{28}\mathrm{Si}$. Again, we find no strong enhancements in the cross section that could be related to states in ^{48}Cr.

Figure 6 shows spectra of excitation energy in ^{28}Si at $E_{\mathrm{lab}}=140$ and 150 MeV, where we now assume that the reaction proceeds via inelastic scattering to a highly excited state in ^{28}Si, which subsequently α decays. These excitation-energy spectra have been generated from the energy and angle of the ^{24}Mg nucleus detected on the opposite side of the beam as the detected α particle. Kinematic focusing of decay α particles from the excited ^{28}Si along the momentum of the decaying fragment thus diminishes the contamination of our ^{28}Si excitation-energy spectra from ^{24}Mg nuclei which are decay products of ^{28}Si. The solid line in Fig. 6 denotes the α-particle decay

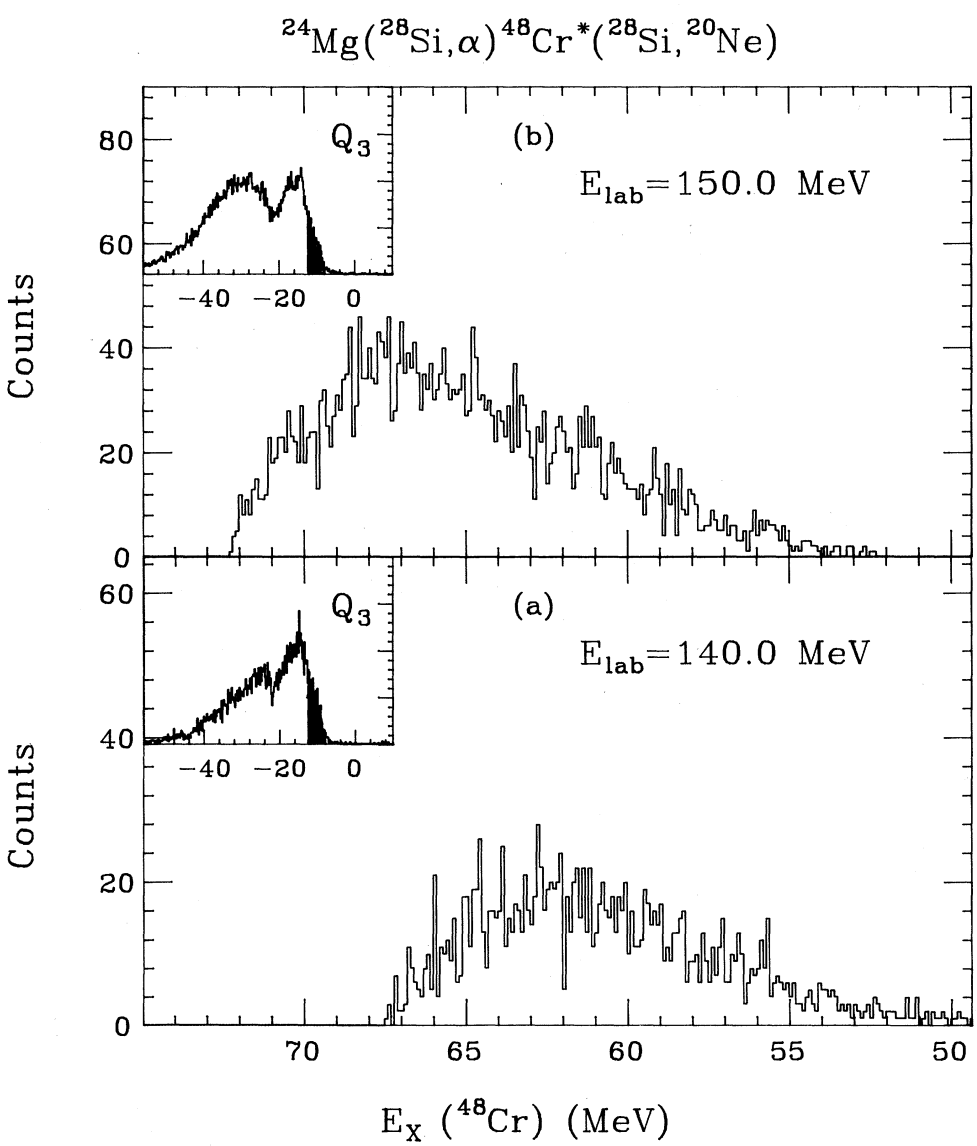

FIG. 5. $E_x(^{48}\mathrm{Cr})$ spectra, for the $\alpha+^{20}\mathrm{Ne}+^{28}\mathrm{Si}$ final states. (a) $E_{\mathrm{lab}}=140$ MeV. (b) $E_{\mathrm{lab}}=150$ MeV. The inserts are the corresponding three-body Q-value spectra for the $\alpha+^{20}\mathrm{Ne}+^{28}\mathrm{Si}$ reaction.

threshold in ^{28}Si. Prominent peaks appear in Fig. 6 near excitation energies of $E_x(^{28}\mathrm{Si})=16.5$ and 20.5 MeV, for both beam energies. Also seen are two somewhat weaker peaks, at excitation energies of 13.0 and 18.0 MeV. In determining the absolute scale of the ^{28}Si excitation energy, an average excitation energy of $E_x(^{24}\mathrm{Mg})=1.37$ MeV was assumed for the primary ^{24}Mg nucleus. This value is simply the average of the excitation energy in the corresponding gate in Q_3. As already discussed, the width of the three-body Q-value window applied to these data contributes to a small ambiguity in the overall scale of the ^{28}Si excitation energy. Also, much of the width of the peaks seen in Fig. 6 may be attributed to the width of the Q_3 gate.

Because of the large amount of angular momentum imparted to the system, we suspect that the observed peaks correspond to high-spin states in ^{28}Si with large α-decay branches to the ground and first-excited states of ^{24}Mg. The density of high-spin states at these excitation energies is presumably much smaller than that of low-spin levels. Therefore, the strong enhancement of only a few levels above the background could be interpreted as reflecting the selectivity of this reaction for the population of such high-spin states. The spectrum of such states at high excitation energy in ^{28}Si is relatively unexplored, however, and these suggestions are merely conjecture at this point.

We now consider the data for the $\alpha+^{20}\mathrm{Ne}+^{28}\mathrm{Si}$ final state. Figure 7 contains spectra of excitation energy in ^{24}Mg derived from the angle and energy of the detected ^{28}Si nucleus. In these spectra, peaks are not as evident as those in the ^{28}Si data. There do appear, however, two

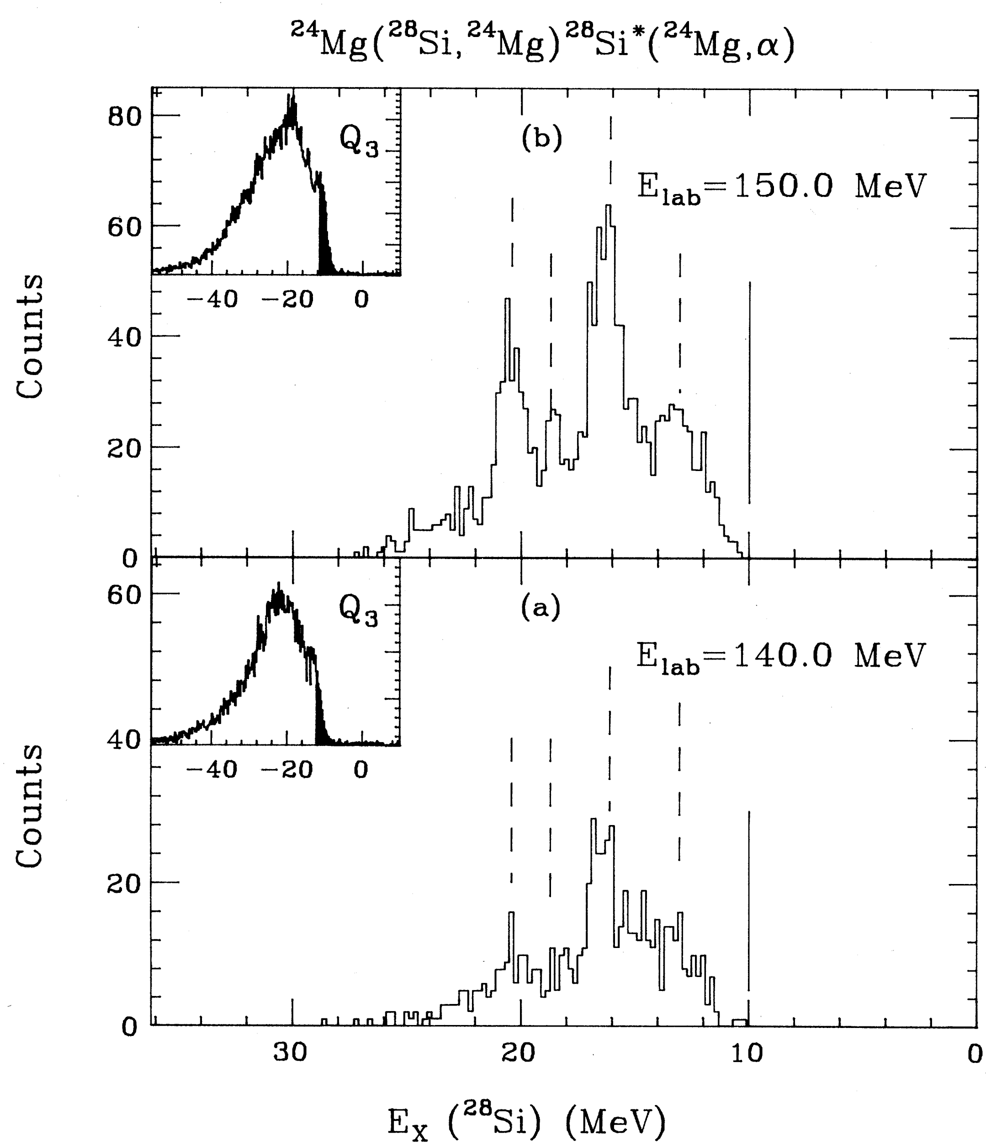

FIG. 6. Excitation-energy spectra for ^{28}Si derived from the angle and energy of one of the two detected ^{24}Mg nuclei for the $\alpha+^{24}\mathrm{Mg}+^{24}\mathrm{Mg}$ final state. (a) $E_{\mathrm{lab}}=140$ MeV. (b) $E_{\mathrm{lab}}=150$ MeV. The line at $E_x=9.982$ MeV indicates the α-particle decay threshold in ^{28}Si. The dashed lines are at excitation energies of $E_x=13.0$, 16.1, 18.7, and 20.4 MeV.

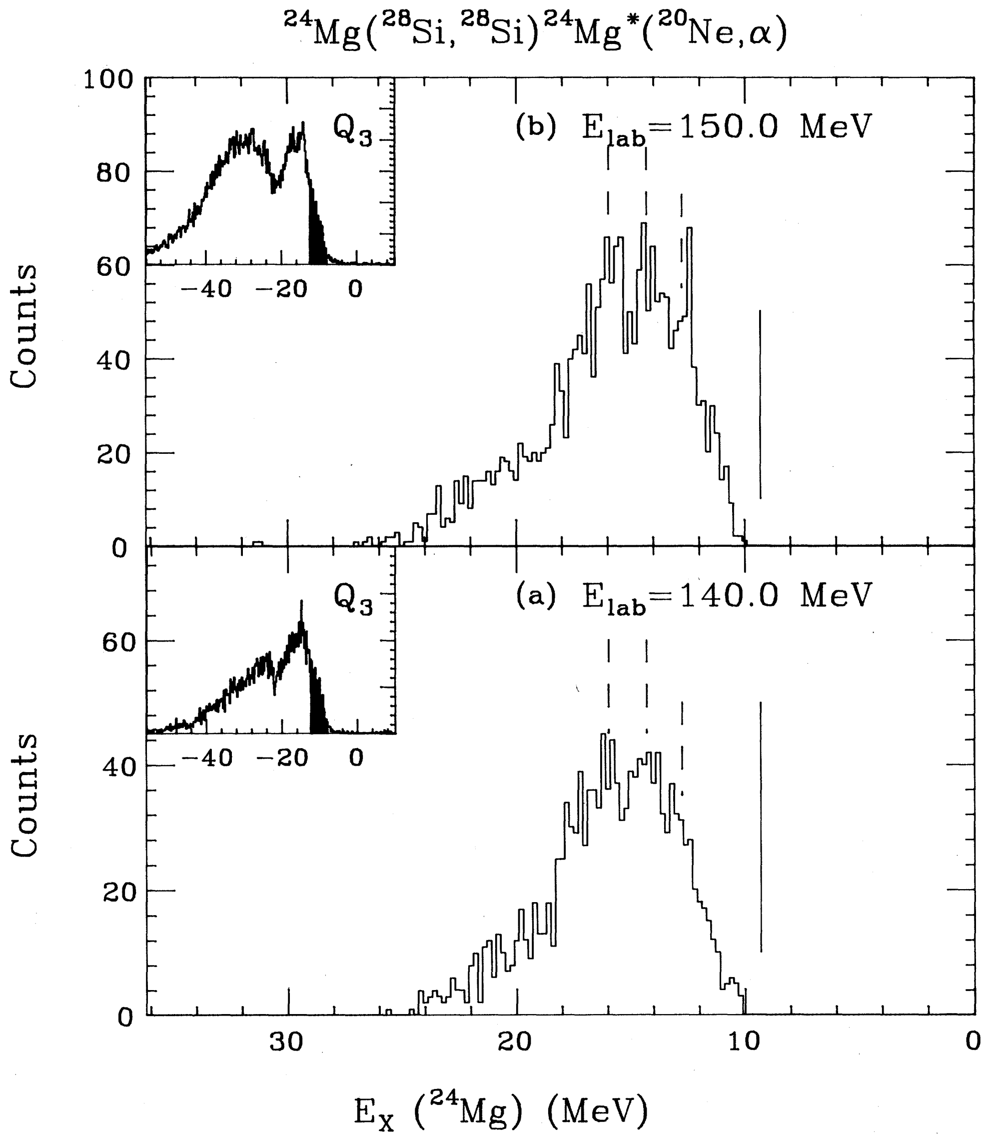

FIG. 7. Excitation-energy spectra for ^{24}Mg, derived from the angle and energy of the detected ^{28}Si nucleus for the $\alpha+^{20}Ne+^{28}Si$ final state. (a) $E_{lab}=140$ MeV. (b) $E_{lab}=150$ MeV. The line at $E_x=9.3$ MeV indicates the α-particle decay threshold in ^{24}Mg. The dashed lines are at $E_x=12.75$, 14.3, and 16.0 MeV.

rather broad states at excitation energies of $E_x=14.3$ and 16.0 MeV, as well as a possible narrow peak at $E_x=12.8$ MeV. The spectrum of ^{24}Mg is quite well known at these excitation energies,[16] with several α-unbound high-spin states occurring at $E_x \geq 12.0$ MeV. As shown in Fig. 7, these structures are quite well correlated in beam energy between $E_{lab}=140$ and 150 MeV. These results suggest that as with the $\alpha+^{24}Mg+^{24}Mg$ reaction, a considerable fraction of the strength leading to the $\alpha+^{20}Ne+^{28}Si$ final state arises from inelastic scattering processes, populating highly excited α-unbound states in ^{24}Mg.

These results quite clearly demonstrate that inelastic scattering mechanisms to α-particle unbound states play an important role in the $^{28}Si+^{24}Mg \rightarrow \alpha+^{24}Mg+^{24}Mg$ and $\alpha+^{20}Ne+^{28}Si$ reactions. The strong excitation of a few states at high excitation energy in the α-decaying heavy ion suggests that these reactions might selectively populate levels of high spin. For the $\alpha+^{24}Mg+^{24}Mg$ final state, we find that a very large fraction, $>75\%$, of the total reaction cross section may be attributed to the population of a few discrete, unbound levels in ^{28}Si. In the $\alpha+^{20}Ne+^{28}Si$ final state, discrete α-decaying levels in ^{24}Mg are also populated, but somewhat less prominently, above a large background. Approximately 15% of the total reaction cross section can be attributed to the population of these levels. The backgrounds observed in the inelastic scattering excitation-energy spectra presumably arise from compound nuclear processes involving the continuum of low-spin levels in the α-decaying nuclei.

We find little evidence for the reactions $^{24}Mg(^{28}Si,\alpha)^{48}Cr^*(^{24}Mg)$ and $^{24}Mg(^{28}Si,\alpha)^{48}Cr^*(^{20}Ne)$, leading to fissioning high-spin levels in ^{48}Cr which correspond to resonances observed in $^{24}Mg+^{24}Mg$ scattering. The level at which these processes occur is apparently weaker than we can detect in this type of experiment. This result, that reactions of this type do not strongly populate fissioning states in the composite system ^{48}Cr, suggests that the study of corresponding states in heavier systems will be quite difficult.

We wish to thank P. F. Lyman and L. E. Seiberling for their assistance in the acquisition of these data. This work was supported by the National Science Foundation.

*Present address: Indiana University Cyclotron Facility, Bloomington, IN 47408.

[1]R. W. Zurmühle, R. R. Betts, S. Saini, F. Haas, and Ole Hansen, Phys. Lett. **129B**, 384 (1983).
[2]R. W. Zurmühle, J. Phys. Soc. Jpn. (Suppl.) **58**, 37 (1989).
[3]R. R. Betts, S. B. DiCenzo, and J. F. Peterson, Phys. Rev. Lett. **43**, 253 (1979).
[4]A. H. Wuosmaa, S. Saini, P. H. Kutt, S. F. Pate, R. W. Zurmühle, and R. R. Betts, Phys. Rev. C **36**, 1011 (1987).
[5]A. H. Wuosmaa, R. W. Zurmühle, P. H. Kutt, S. F. Pate, S. Saini, M. L. Halbert, and D. C. Hensley, Phys. Rev. Lett. **58**, 1312 (1987).
[6]S. Saini, R. R. Betts, R. W. Zurmühle, P. H. Kutt, and B. K. Dichter, Phys. Lett. B **185**, 316 (1987).
[7]P. H. Kutt, S. F. Pate, A. H. Wuosmaa, R. W. Zurmühle, Ole Hansen, R. R. Betts, and S. Saini, Phys. Lett. **155B**, 27 (1985).
[8]R. R. Betts, in *Nuclear Physics with Heavy Ions,* edited by P. Braun-Munzinger (Harwood, New York, 1984).
[9]K. Nagatani, T. Shimoda, D. Tanner, R. Tribble, and T. Yamaya, Phys. Rev. Lett. **43**, 1480 (1979).
[10]A. J. Lazzarini, S. G. Steadman, R. J. Ledoux, A. Sperduto, G. R. Young, K. van Bibber, and E. R. Cosman, Phys. Rev. C **27**, 1550 (1983).
[11]W. D. Rae, R. G. Stokstad, B. G. Harvey, A. Dacal, R. Legrain, J. Mahoney, M. J. Murphy, and T. J. M. Symons, Phys. Rev. Lett. **45**, 884 (1980).
[12]R. Wieland, R. Stockstad, A. Gobbi, D. Shapira, L. Chua, M. W. Sachs, and D. A. Bromley, Phys. Rev. C **9**, 1474 (1974).
[13]R. W. Zurmühle and L. Csihas, Nucl. Instrum. Methods **203**, 262 (1982).
[14]R. H. Dalitz, Phys. Rev. **94**, 1046 (1954).
[15]K. Swiek-Wilczynska, J. Wilczynski, C. R. Albiston, Y. Chan, E. Chavez, S. B. Gazes, H. R. Schmidt, and R. G. Stokstad, Phys. Rev. C **35**, 1316 (1987).
[16]L. K. Fifield, R. W. Zurmühle, and D. P. Balamuth, Phys. Rev. C **8**, 2217 (1974).